Proc. Int. Symp. Fe-Pnictide Superconductors
J. Phys. Soc. Jpn. **77** (2008) Suppl. C, pp. 84-86

Paramagnetic properties of $NdFeAsO_{0.94}F_{0.06}$ polycrystals

C. TARANTINI[1], A. GUREVICH[1], F. KAMETANI[1], A. YAMAMOTO[1], D.C. LARBALESTIER[1], Z.A. REN[2], X.L. DONG[2], W. LU[2] and Z.X. ZHAO[2]

[1]*National High Magnetic Field Laboratory, Florida State University, Florida, 32310 USA*

[2]*National Laboratory for Superconductivity, Institute of Physics and Beijing National Laboratory for Condensed Matter Physics, Chinese Academy of Sciences, P.O. Box 603, Beijing 100190, P.R. China*

(Received August 15, 2008)

The temperature and field dependencies of magnetization of $NdFeAsO_{0.94}F_{0.06}$ bulk sample are shown to exhibit the Curie-Weiss behaviour, both in the superconducting and normal states. To address the origin of the strong paramagnetic signal, particularly to reveal contributions from antiferromagnetic second phases in sintered $NdFeAsO_{0.94}F_{0.06}$, the magnetic response of Nd_2O_3 was measured and compared with $NdFeAsO_{0.94}F_{0.06}$. Our measurements show that paramagnetism of $NdFeAsO_{0.94}F_{0.06}$ is an intrinsic property dominated by Nd^{3+} ions contribution, which cannot be explained by magnetic second phases.

KEYWORDS: High-T_c superconductivity, Fe-based oxypnictides, magnetic properties, paramagnetism, antiferromagnetism.

1. Introduction

The recent discovery of superconductivity in the oxypnictides has stimulated an enormous interest in this class of materials.[1-4] The *RE*FeAsO (*RE*=La, Pr, Ce, Sm, Nd) compounds have layered structures formed by insulating *RE*O and conducting FeAs planes. Upon electron or hole doping, oxypnictides exhibit an unusual coexistence of high superconducting critical temperatures T_c = 26-57 K with strong antiferromagnetic (AF) correlations and extremely high upper critical fields.[5] Neutron,[6,7] μSR,[8,9] and NMR[10,11] studies of undoped parent compounds have revealed a spin density wave instability on FeAs planes at T_N ~140-150 K accompanied by a drop in the normal state resistivity and orthorhombic distortions of the tetragonal lattice.[3] Doping with fluorine or oxygen reduces T_N and seemingly eliminates manifestations of these transitions in ρ(T) of optimally doped oxypnictides.[12,13]

In a recent work[14] we studied the magnetic properties of $NdFeAsO_{0.94}F_{0.06}$ in a wide range of temperature and high magnetic fields up to 33 T. It was shown that this compound has a strong paramagnetic behaviour both below and above the critical temperature. In particular, we found that in normal state the magnetization M = χ(T)H exhibits a Curie-Weiss behaviour, $\chi(T) = C/(T + T_N)$ with a Neel temperature T_N ~11-12 K. However, the measurements of M(H,T) performed below T_c have shown the lack of the long-range AF order in $NdFeAsO_{0.94}F_{0.06}$, which can be regarded as a paramagnetic superconductor similar to $Nd_{1.85}Ce_{0.15}CuO_4$[15]. Given that the sintered $NdFeAsO_{0.94}F_{0.06}$ has several AF second phases, like Nd_2O_3, Fe_2As, FeAs and $FeAs_2$, the important question is if the observed paramagnetism is an intrinsic property of the superconducting phase or it comes from the magnetic second phases. In this work we address this issue by comparing the magnetic response of the superconducting $NdFeAsO_{0.94}F_{0.06}$ with that of Nd_2O_3 powder. We show that in both cases the paramagnetism is dominated by the Nd^{3+} ions. However, the observed paramagnetism is so strong that it can only be explained assuming that it is indeed the intrinsic property of the superconducting $NdFeAsO_{0.94}F_{0.06}$ phase but is not entirely determined by magnetic second phases.

2. Experimental details and results

The polycrystalline $NdFeAsO_{0.94}F_{0.06}$ bulk samples were synthesized by solid state reaction under high pressure as described in Ref.[16]. Powders of NdAs, Fe, Fe_2O_3, FeF_2 were mixed together according to the nominal stoichiometric ratio then ground and pressed into small pellets. Then they were sealed in boron nitride crucibles and sintered in a high pressure synthesis apparatus under the pressure of 6 GPa at 1250°C for 2 hours. The critical temperature of the sample is about 49 K.

Microstructural analysis was performed using field emission scanning electron microscope (Carl Zeiss 1540

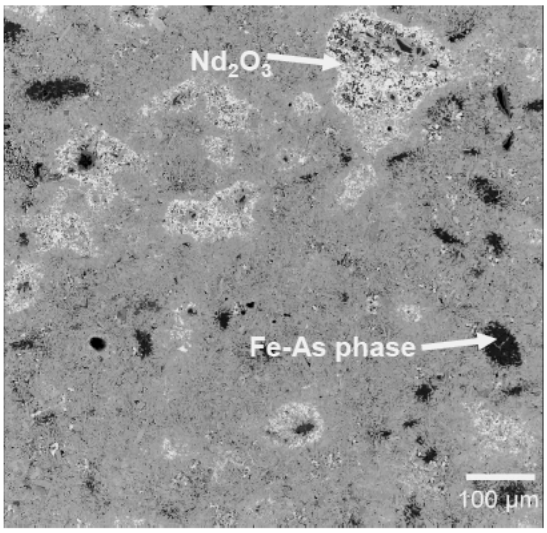

Fig. 1. SEM image of $NdFeAsO_{0.94}F_{0.06}$ polycrystalline sample. The arrows point at the impurity phases, Nd_2O_3 and Fe-As glassy phases.

ESB), while magnetic moment of both $NdFeAsO_{0.94}F_{0.06}$ and Nd_2O_3 was performed by a SQUID magnetometer (Quantum Design: MPMS-XL5s).

Figure 1 shows the scanning electron microscopy (SEM) image of the $NdFeAsO_{0.94}F_{0.06}$ bulk sample, which has about 90% of the theoretical density. Atomic number sensitive backscattering electron imaging reveals a multi-phase microstructure, which contains both the superconducting phase (intermediate grey contrast) and about 20% of non-superconducting second phases: in particular Nd_2O_3 (white contrast) and Fe-As glassy phases (dark contrast) as identified by EDS. These glassy phases comprise three main AF phases: Fe_2As, FeAs, and $FeAs_2$, which have the Neel temperatures of 353, 77 and <5K, respectively[17]. The volume fraction of these phases is typically about few per cents, yet the AF transition in $FeAs_2$ may manifest itself in a peak in the specific heat in the superconducting state at low temperatures, T ≈ 3-5K.

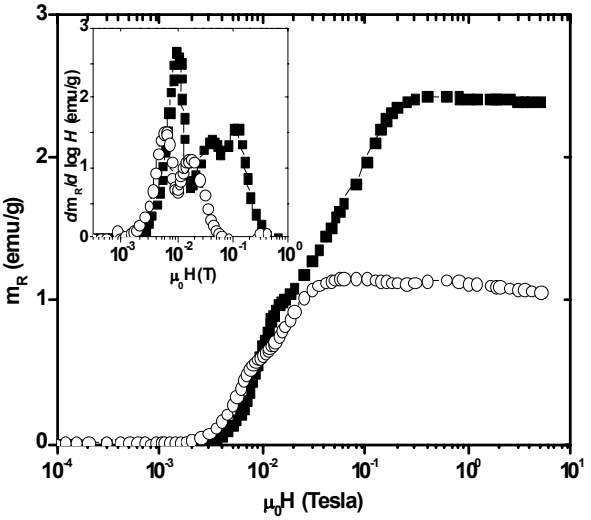

Fig. 2. Remnant magnetization (m_R) as a function of the maximum applied field at 5 (full symbols) and 20 K (open symbols) for $NdFeAsO_{0.94}F_{0.06}$. Several peaks in the derivative $dm_R/d\log H$ shown in the inset indicate multiple scales of magnetization current flow.

The multiphase structure of our sintered sample shown in Fig. 1 can result in magnetic granularity effects, which can manifest themselves in a double-shoulder field dependence of the remnant magnetization $m_R(H)$ in the superconducting critical state as a function of the applied magnetic field[18]. This behavior is illustrated in Fig. 2 for two different temperatures. Here the peaks in the derivative $dm_R/d\log H$ shown in the inset correspond to intergranular and intragranular penetration fields, indicating multiple scales of magnetization current loops.

Fig. 3 shows the temperature dependencies of the magnetization m(T,H) of $NdFeAsO_{0.94}F_{0.06}$ and Nd_2O_3 powder for two different fields, 0.5 and 2 T. For the superconducting sample, both zero-field-cooled (ZFC) and field-cooled (FC) magnetizations were measured. Both Nd_2O_3 and $NdFeAsO_{0.94}F_{0.06}$ in the normal state exhibit the typical Curie-Weiss paramagnetic behaviour. In order to directly compare magnetic response of these two materials, we normalized their respective magnetizations m(H,T) per single Nd^{3+} ion. In the normal state not only are the temperature dependencies of the so-normalized m(T,H) very

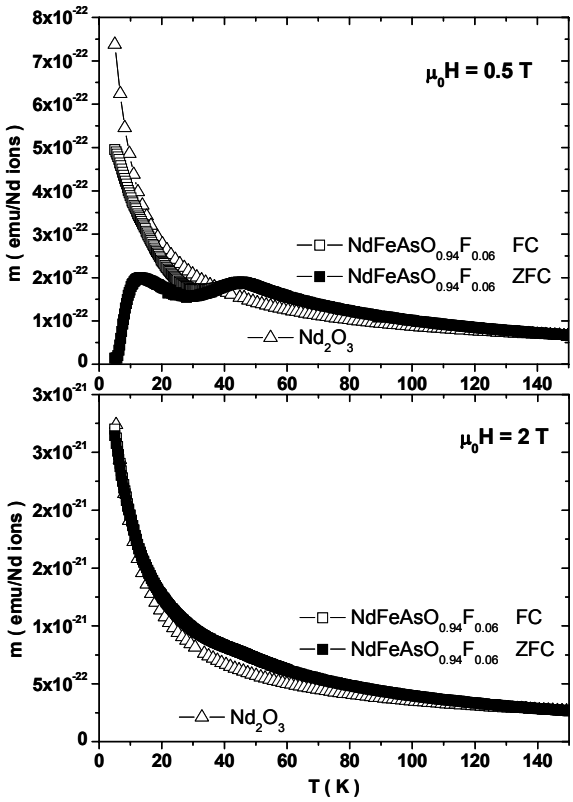

Fig. 3. Temperature dependencies of magnetic moments per single Nd ion for both $NdFeAsO_{0.94}F_{0.06}$ (ZFC, full square symbols; FC, open square symbols) and Nd_2O_3 (open triangular symbols) at two different applied field.

similar, the absolute values of m(T,H) become very close as well. This result unambiguously indicates that the observed paramagnetism can only come from Nd^{3+} ions, the only magnetic ion in the neodymium oxide. The data in Fig. 3 also show that paramagnetism of $NdFeAsO_{0.94}F_{0.06}$ below T_c is reduced by diamagnetic magnetization currents produced by pinned vortices in the superconducting critical state.

Fig. 4 shows the magnetization loop for $NdFeAsO_{0.94}F_{0.06}$ in the superconducting state superimposed onto the magnetization of Nd_2O_3, both being normalized per single Nd^{3+} ion. Magnetization of $NdFeAsO_{0.94}F_{0.06}$ below T_c exhibits the superconducting hysteresis loop on top of a strongly paramagnetic, field-dependent background. Taking the mean value of the ascending and descending branches of m(B), we define the paramagnetic magnetization, $m_p = (m_\uparrow + m_\downarrow)/2$ where the arrows indicate the magnetic field direction. The width of the magnetization hysteretic loop, $\Delta m = m_\uparrow - m_\downarrow$ is proportional to the critical current density in the Bean model. As follows from Fig. 4, the magnetization per Nd ion for Nd_2O_3 fits right between the upper and lower branches of the hysteretic loop for $NdFeAsO_{0.94}F_{0.06}$. These data show basically identical paramagnetic behaviours of these two materials below T_c, in the same way as the data shown in Fig. 3 do for the high-temperature Curie-Weiss magnetization in the normal state. The results presented above show that the strong paramagnetism of $NdFeAsO_{0.94}F_{0.06}$ is dominated by Nd^{3+} ions while possible contributions of AF second phases can only account for a few percent of the observed m(T,H).

Indeed, if the strong paramagnetism of $NdFeAsO_{0.94}F_{0.06}$ is determined by only AF second phases, the magnetic

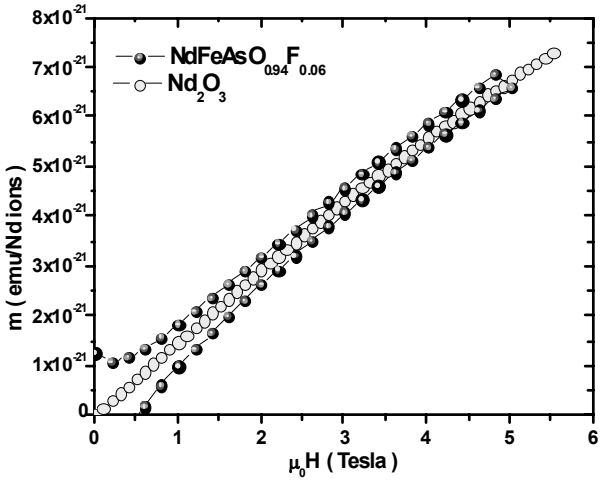

Fig. 4. Magnetic moment normalized at the Nd ion content of $NdFeAsO_{0.94}F_{0.06}$ polycrystalline sample (black symbols) and of Nd_2O_3 (open symbols) as a function of applied magnetic field at 5 K.

moment per Nd^{3+} ion should be much smaller than the signal observed for the pure Nd_2O_3 just because all AF second phases amounts to less than 20% of the sample volume. However, Figs. 3 and 4 clearly show that the paramagnetic responses of $NdFeAsO_{0.94}F_{0.06}$ and Nd_2O_3 per Nd^{3+} ion are nearly identical. This means that every Nd^{3+} ion in our sample contributes to the paramagnetic signal, no matter if it is in the superconducting phase or in the oxide. Such similar paramagnetic behaviour of Nd_2O_3 and $NdFeAsO_{0.94}F_{0.06}$ can be understood given that $NdFeAsO_{0.94}F_{0.06}$ contains alternating FeAs and NdO layers, the later being basically a "built in" Nd oxide multilayer component with the same NdO octahedral arrangement as in Nd_2O_3. As a result, the paramagnetic behaviour of $NdFeAsO_{0.94}F_{0.06}$ is similar to that of many Nd-based compounds [19] like Nd_2O_3, $NdGaO_3$, $NdGaO_3$, $La_{1.6-x}$ $Nd_{0.4}$ $Sr_xCuO_{4-\delta}$, Nd_2CuO_4, Nd_2BaCuO_5 in which crystal electric field results in a significant reduction of the magnetic moment of Nd ions from $3.62\mu_B$ for the free Nd^{3+} ion down to $0.7\text{-}1.5\mu_B$, as we also observed in our high field measurements [14].

Given that the magnetic moment ($\approx 0.25\text{-}0.35\mu_B$) of Fe^{2+} is significantly smaller than the moment of Nd^{3+} ions, paramagnetic contribution of superconducting FeAs planes to the magnetization of $NdFeAsO_{0.94}F_{0.06}$ is likely to be much smaller than the contribution from Nd^{3+}. Moreover, possible paramagnetic contributions from Fe-As second phases below T_c are greatly reduced because the Neel temperatures of Fe_2As, and FeAs are higher than T_c, while the volume fraction of $FeAs_2$ with $T_N < 5K$[17] is certainly much smaller that of Nd^{3+} ions.

3. Conclusions

The magnetic properties of $NdFeAsO_{1-x}F_x$ member of the new family of recently discovered superconducting oxypnictides are quite peculiar. This material has a strong paramagnetic behaviour coexisting with superconductivity that cannot be ascribed to AF second phases. In fact, the comparison of the field dependence of the magnetic moment at low temperature for $NdFeAsO_{0.94}F_{0.06}$ and one of the main second phases, Nd_2O_3 clearly shows that the paramagnetic background in the superconducting sample normalized per a single Nd^{3+} ion is comparable to the oxide response. This means that the magnetization is determined by Nd^{3+} ions, no matter what phase they are in. Because the temperature dependencies of the magnetization in these two compounds are similar, strong paramagnetism observed in the $NdFeAsO_{0.94}F_{0.06}$ cannot result from Fe-As phases. Thus, $NdFeAsO_{0.94}F_{0.06}$ can be regarded as a paramagnetic superconductor in which superconductivity and paramagnetism coexist on different FeAs and NdO planes.

Acknowledgment

The work at NHMFL was supported by the NSF grant DMR-0084173 with support from the state of Florida and AFOSR.

1) Y. Kamihara, T. Watanabe, M. Hirano, and H. Hosono. J. Am. Chem. Soc. **130**, 3296 (2008).
2) X. H. Chen *et al.*, *Nature* **453**,761-762 (2008) .
3) G. F. Chen *et al.*, Phys. Rev. Lett. **100**, 247002 (2008)
4) Z. A. Ren, cond-mat:0803.4283v1 (2008).
5) F. Hunte *et al.,* Nature **453**, 903 (2008).
6) C. de la Cruz *et al.,* Nature **453**, 899 (2008).
7) Y. Chen *et al.,* ArXiv:0807.0662.
8) A.J. Drew *et al.,* ArXiv:0805.1042v1.
9) A.A. Aczel *et al.* ArXiv:0807.1044.
10) K. Ahilan *et al.,* ArXiv:0804.4026v1.
11) Y. Nakai *et al.,* ArXiv:0804.4765v1.
12) H.-H. Wen *et al.,* Europhys. Lett. **80**, 17009 (2008).
13) A.S. Sefat *et al.,* Phys. Rev. B **77**, 174503 (2008).
14) C. Tarantini *et al.*, ArXiv:0805.4445.
15) J.W. Lynn, *et al*., Phys. Rev. B**41**, 2569(R) (1990); M. Matsuura *et al*., Phys. Rev. B**68**, 144503 (2003); Phys. Rev. **69**, 104510 (2004).
16) Z.A. Ren *et al.* Europhys. Lett. **82**, 57002 (2008).
17) M. Yuzuri, R. Tahara, and Y. Nakamura. J. Phys. Soc. Japan **48**, 1937 (1980).
18) A. Yamamoto *et al.,* Supercond. Sci. Technol. **21**, 095008 (2008).
19) M. Faucher *et al*., Phys. Rev. B **21** 3689 (1980); S. Jandl et al., Phys. Rev. B**65**, 11600 (1997); Podlesnyak *et al.,* J. Phys. Cond. Mat. 5, 89731 (1993); G. Rou et al, Phys. Rev. B **66**, 224508 (2002); P. Dufour *et al.,* Phys. Rev. B**51**, 1053 (1997); A.T. Boothroyd *et al.*, Phys. Rev. B**45**, 10075 (1992); R.S. Puche *et al.,* Phys. Rev. B**71**, 024403 (2005).